JPE 11-3-2

Primary Current Generation for a Contactless Power Transfer System Using Free Oscillation and Energy Injection Control

Hao Leo Li†, Aiguo Patrick Hu*, and Grant Anthony Covic*

†* Dept. of Electrical and Computer Eng., University of the Auckland, Auckland, New Zealand

Abstract

This paper utilizes free oscillation and energy injection principles to generate and control the high frequency current in the primary track of a contactless power transfer system. Here the primary power inverter maintains natural resonance while ensuring near constant current magnitude in the primary track as required for multiple independent loads. Such energy injection controllers exhibit low switching frequency and achieve ZCS (Zero Current Switching) by detecting the high frequency current, thus the switching stress, power losses and EMI of the inverter are low. An example full bridge topology is investigated for a contactless power transfer system with multiple pickups. Theoretical analysis, simulation and experimental results show that the proposed system has a fast and smooth start-up transient response. The output track current is fully controllable with a sufficiently good waveform for contactless power transfer applications.

Key Words: Contactless power transfer, Energy injection control, Multiple pickups, Resonant inverter, Soft switching

I. Introduction

A typical contactless power transfer system employs a power converter to produce a high frequency current along a track loop/coil for magnetic field generation. The generated magnetic field loosely couples the primary track loop/coil and secondary pickup coil(s) to enable power transfer from a primary platform to secondary movable loads without cable connection. Due to the elimination of physical electrical contact, such a power transfer system is preferred in many hazardous and clean environments as it eliminates sparking, particles and the risk of electrical shock. As such, it has been successfully employed in many applications, including materials handling systems, transportation, bio-medical implants, semi-conductor manufacturing workshops, battery chargers, etc [1]–[5].

Fig.1 shows a typical configuration of a contactless power transfer system with multiple independent loads. As shown, the stationary primary side includes a high frequency power inverter and a compensated conductive track loop/coil for the generation of a high frequency ac current. The secondary side consists of a number of compensated pickups and rectification circuits to drive each independent load. They are coupled over the part of the track/coil in which the pickup inductor (coil and magnetic material) is present via the magnetic field generated by the primary side.

Manuscript received Oct. 20, 2010; revised Feb. 24, 2011
Recommended for publication by Associate Editor Byung-Cho Choi.
† Corresponding Author: hli076@aucklanduni.ac.nz
Tel: +64-21-033-3307, Fax: +64-9-9148310, University of Auckland
* Dept. of Electrical and Electronics Eng., University of Auckland, New Zealand

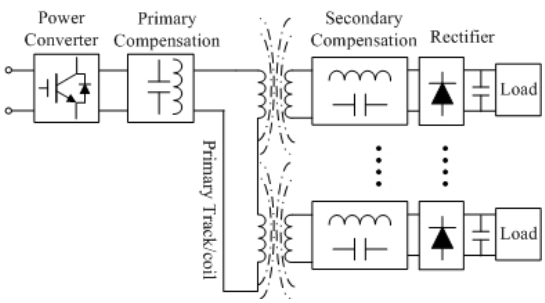

Fig. 1. Typical configuration of a contactless power transfer system with multiple pick-ups.

Power inverters employed in contactless power transfer systems are either voltage or current fed [6], [7]. To generate a high frequency current on the primary track suitable for various applications, the switching frequency of an inverter based on traditional voltage or current fed inversion methods has to be close or equal to the actual frequency of the current due to the forced switching operation [8]–[11]. Owing to the forced switching nature, the circuit transient process involved in those power inverters is normally complex and difficult to analyze [11]–[13]. In consequence, unpredicted voltage or current overshoots during start-up and load transients may damage the switching devices or other components [14]–[16].

Integral cycle mode controlled inverters, also later named as quantum resonant inverters [17], [18], have been proposed for dc-dc conversion. Although such inverters could be used to generate high frequency ac current based on cycle sequence ratio of the powering, free ringing and regeneration modes,

the control objective of these inverters was to keep the output dc voltage constant. In practice, the control dynamics of such systems are relatively slow and dominated by the output filter so that the magnitude of the high frequency transformer ac current can have severe fluctuations without affecting the control objectives. Such a control approach is unsuitable in a contactless power transfer application where multiple pickups exist with highly variable loads. In such systems, the magnitude of the high frequency primary current needs to be maintained nominally constant to ensure each power pickup can operate independently without compromising the power transfer.

This paper utilizes a dc-ac inversion method based on discrete energy injection and free oscillation. The objective is to generate and control the magnitude of the high frequency current along the track/coil for contactless power transfer. Because the primary current magnitude reflects the stored energy in the resonant circuit, it can be controlled to be constant at a preset value by controlling the energy injection, regardless of the output demands of power pickups and loads. In practice, each pickup will normally have its own controller to regulate the output. Compared to traditional voltage and current fed dc-ac inversion methods, the proposed method can be used to generate a high frequency primary current for a contactless power transfer system that operates with a reduced switching operation under most loading conditions, since the average load is normally below the peak capacity of the supply. As such, the proposed method is not as constrained by the switching frequency limitations of the semiconductor devices. Many different topologies may be developed based on the basic inversion concept proposed. In this paper, a full bridge inverter is developed as an example.

The paper is organized in the following order: Section II presents the basic concept of the proposed inversion method first. A full bridge energy injection inverter example is analysed in Section III, and then a detailed controller design of the proposed dc-ac inverter is described in Section IV. Section V presents theoretical analysis of the worst-case primary current ripple under energy injection control. Section VI gives the experimental results. Finally, conclusions are drawn in Section VII.

II. Basic Concept of Energy Injection and Free Oscillation

A principle diagram of the inversion method based on discrete energy injection and free oscillation control is shown in Fig. 2. It comprises a dc power supply, a switching network and a series resonant circuit consisting of a lumped inductor L, a capacitor C, and an equivalent resistor R_{eq}. The effect of power pickups can be considered by calculating the total the reflected impedance summed from each of the secondary sides of the contactless power transfer system [19].

There are two individual operating modes for the dc-ac inversion shown in Fig. 2: energy injection and free oscillation. When the terminals a and b are shorted by the switching network, the track inductor L, its tuning capacitor C and the equivalent resistor R_{eq} form a free oscillation network,

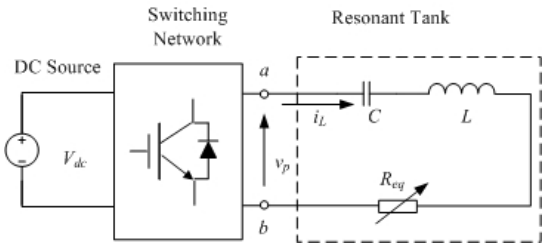

Fig. 2. Principle diagram of the energy injection and free oscillation inverters.

which is decoupled from the power supply. In principle, if there are no power losses in the resonant tank, the circuit can oscillate infinitely without need of energy injection. However, in practice power consumption always exists because of the various ESRs (Equivalent Series Resistances) in the system and additionally from the load when presents [20]. When more energy is required, the inverter is reconfigured to supply power into the resonant tank. Such operation is very different from normal voltage or current fed inverters.

The switching network can be designed to control the energy injection in either one or both direction of the resonant current. As such, either half bridge, full bridge or other suitable topologies could be developed as design options. The unique feature of the inversion method lies in the control of the resonant current to ensure proper energy injection into the network if required. The inverters can be hard or soft switched, but the basic rule is that the energy injection should be able to compensate for the power losses promptly and smoothly without significantly affecting the circuit oscillation parameters, such as the frequency and magnitude of the primary current. Regardless of the switching conditions of the inverter, the input voltage to the resonant tank can be defined as:

$$v_p(t) = \begin{cases} V_{dc} & \text{(Positive Energy Injection)} \\ -V_{dc} & \text{(Negative Energy Injection)} \\ 0 & \text{(Free Oscillation)} \end{cases}. \quad (1)$$

According to Kirchhoff's voltage law (KVL), the following differential equations can be obtained under both the energy injection and free oscillation conditions as:

$$\begin{cases} \dfrac{di_L}{dt} = \dfrac{1}{L}(v_p - v_c - R_{eq} i_L) \\ \dfrac{dv_c}{dt} = \dfrac{1}{C} i_L \end{cases}. \quad (2)$$

No matter whether the system operates in either mode, from (2) a differential equation expressed in terms of the track current can be expressed as:

$$LC\frac{d^2 i_L}{dt^2} + R_{eq} C\frac{di_L}{dt} + i_L = 0. \quad (3)$$

During the free oscillation period, the full solution to the track current can be found as:

$$i_L = \frac{-v_C(0)}{\omega L} e^{-\frac{t}{\tau}} \sin \omega t + i(0)\frac{\omega_0}{\omega} e^{-\frac{t}{\tau}} \cos(\omega t + \theta) \quad (4)$$

where $v_C(0)$ and $i_L(0)$ are the initial voltage of the tuning capacitor C and the initial current of the track inductor respectively. $\tau = 2L/R_{eq}$ is the time constant of resonant circuit, reflecting the decay of the track current envelope (theoretically

if R_{eq}=0, then $\tau = \infty$, there would be no decay), The oscillation frequency of the track current is determined by the track loop/coil parameters under normal operating conditions. As long as the system does not enter bifurcation [21], it is governed by the following equation:

$$\omega = \omega_0 \sqrt{1-\zeta^2}. \tag{5}$$

where ω_0 is the undamped natural frequency $\omega_0 = 1/\sqrt{LC}$, ζ is the damping factor of the network, which can be expressed as: $\zeta = R_{eq}/2\sqrt{L/C} = 1/2Q$, and the phase shift θ in (4) can be expressed as: $\theta = \arctan(1/\omega\tau) = \arctan(\zeta)$. It can be seen that to make the network oscillation occur, $Q > 0.5$, otherwise the circuit will be over damped. A high Q primary will help to stable the current as it naturally stores more energy, as such the switching frequency required to maintain the oscillation in the primary is much lower when an energy injection controller are used.

If the zero current switching (ZCS) is achieved, then the initial current $i_L(0)$ is zero, and the corresponding initial voltage of the tuning capacitor $v_C(0)$ will be around its peak value. Under such a condition, the second term of (4) becomes zero, resulting in a simple current equation given by:

$$i_L = \frac{v_C(0)}{\omega L} e^{-\frac{t}{\tau}} \sin \omega t. \tag{6}$$

When the positive or negative half cycle track current flows through the voltage source in the same direction (for positive and negative energy injection respectively), the track current can be expressed as:

$$i_L = \frac{v_p + v_C(0)}{\omega L} e^{-\frac{t}{\tau}} \sin \omega t \tag{7}$$

where v_p has been defined in (1). The amount of injected energy in each half cycle is determined by the magnitude of the input dc voltage and the track/coil current, as well as the injection period:

$$E_{in} = \int_0^{\Delta t} v_p(t) i_L(t) dt \tag{8}$$

where Δt is the time period of the energy injection.

III. A Full Bridge Inverter

Fig. 3 shows the operation states of a simple full bridge topology. It can be seen that the basic structure is not much different to a conventional full bridge voltage fed resonant inverter, but the control strategy is very different. The operation of the switches is to simply maintain constant energy in the primary track/coil. If only two upper switches S_1+, S_2+ are turned "off" and meanwhile two lower S_1-, S_2- are turned "on", the fully charged C will discharge in either the positive or negative direction, thus a free oscillation path is formed for the track current. At each injection period, S_1+, S_2- is controlled to be "on"(S_2+, S_1- "off") in positive cycle of the resonant current; or S_2+, S_1- is "on"(S_2+, S_1- "off") in the negative cycle of the resonant current. During the energy injection period the resonant circuit is then connected to the power source V_{dc} with the current flowing in the same direction, so that the energy is brought into the network. If sufficient energy is brought into the resonant tank in a fast and efficient manner to replace the consumed energy, the resonant current in the track will be maintained at the free oscillation frequency. Therefore, the total electromagnetic energy of the resonant tank can be maintained and controlled.

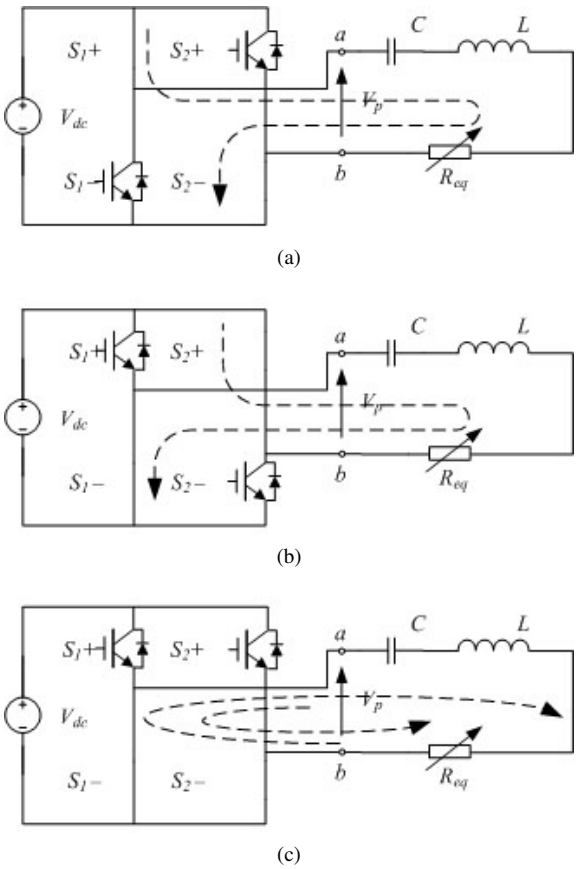

Fig. 3. Basic operating states of the inverter. (a) Energy injection state in positive cycle of resonant current. (b) Energy injection state in negative cycle of resonant current. (c) Free oscillation state.

The advantage of such a full bridge topology is simply that it can control the energy injection in both the positive and negative directions of the track current. As such, the power range that can be controlled by a full bridge topology is broader than a half bridge topology. Furthermore, the full bridge topology enables a faster dynamic response during start-up or load variations.

If energy injection occurs at each positive half cycle of the current, then the voltage exerted to the track loop/coil reaches its maximum value with a fundamental magnitude given by:

$$V_{rms} = \frac{2}{\pi\sqrt{2}} V_{dc}. \tag{9}$$

The maximum power that can be supplied by a dc voltage source is achieved if energy is injected in each positive and negative cycle, and can be expressed by:

$$P_{max} = \frac{V_{rms}^2}{R_{eq}} = \frac{8}{\pi^2} \frac{V_{dc}^2}{R_{eq}}. \tag{10}$$

IV. Control Strategy

A controller is developed in this section for the full bridge inverter. Due to the nature of free oscillation and discrete

TABLE I
BASIC CONTROL STATES OF A FULL BRIDGE INVERTER

Energy injection							
$i(t)>0, \hat{i}/pre\frac{T}{2}<+I_{ref}$				$i(t)<0, \hat{i}/pre\frac{T}{2}<-I_{ref}$			
S1+	*S1-*	*S2+*	*S2-*	*S1+*	*S1-*	*S2+*	*S2-*
On	off	on	off	on	off	on	off
Free oscillation							
$i(t)>0, \hat{i}/pre\frac{T}{2}>+I_{ref}$				$i(t)<0, \hat{i}/pre\frac{T}{2}>-I_{ref}$			
S1+	*S1-*	*S2+*	*S2-*	*S1+*	*S1-*	*S2+*	*S2-*
off	on	off	on	off	on	off	on

energy injection control, the operating period of the switches S_1+ and S_2+ is constrained by the direction of the track current and the requirement of the energy level.

The actual ZCS frequency of full bridge inverter is not necessarily equal to the nominal natural resonant frequency of the oscillation circuit. In consequence, fixed switching frequency controller is unable to follow the actual resonant frequency variation during operation, consequently the switches can experience high voltage/current stresses, as well as high power losses and EMI when the load varies or the circuit parameters drift [21]. This paper focuses on soft switching control realized by ZCS operation. A variable frequency control method is proposed and developed here to allow frequency variations. If the contactless power transfer system is properly designed with a large equivalent primary circuit quality factor Q (with the reflected components from secondary side taken into consideration), the actual frequency variation is very small during practical operation.

A. Soft switched start-up

Owing to the circuit resonance, the operation of the inverter can follow the resonance of the track current. Initially, all switches are in their "off" state; there is no electric and magnetic energy stored in the track loop/coil. The voltage across C and the current in the track loop/coil are all zero. When S_1+, S_2- are controlled "on"; and S_2+, S_1- are controlled "off", the source voltage (V_{dc}) is applied to the resonant loop/coil and energy is injected into the track in the positive half cycle. After C is fully charged, a free oscillation path for the current is formed, if S_1+, S_2+ are controlled "off" and S_2-, S_1- are turned "on". The current then oscillates freely in the track. In this start-up transient process, all switches naturally operate in ZCS condition.

B. Steady-state operation

A control strategy that uses the current as the control variable to achieve ZCS operation is proposed. If the track current in a previous half cycle is smaller than a predefined current reference, energy injection will be controlled to occur in the next half cycle. Otherwise, if the peak current in the previous half cycle is larger than the predefined reference, the free oscillation of the resonant circuit will be maintained. The control strategy with reference to the track current is illustrated in Fig. 4. The detailed control of the inverter switches under this strategy is shown in Table I. The flow chart of the control algorithm is shown in Fig. 5.

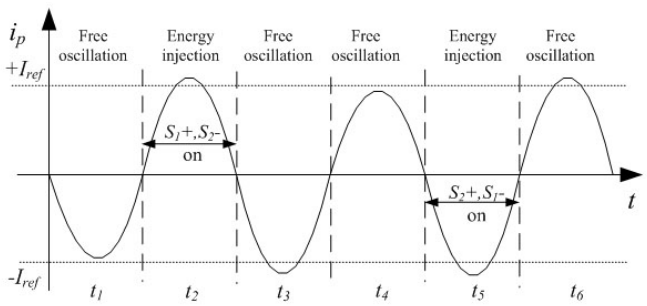

Fig. 4. Steady-state ZCS energy injection control strategy.

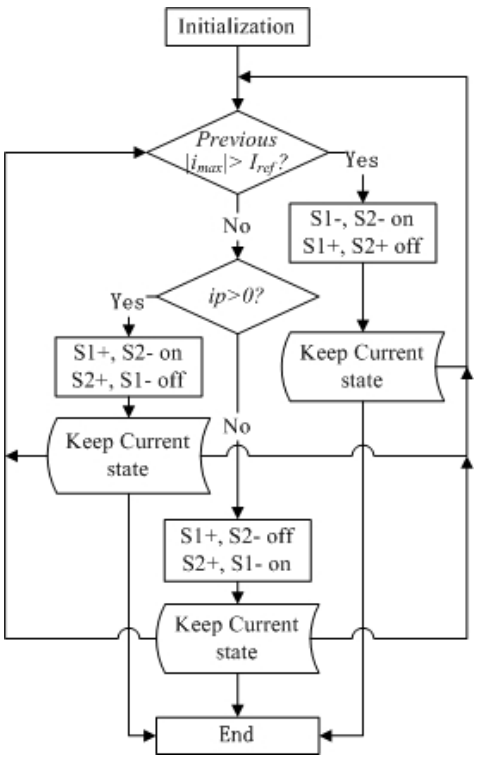

Fig. 5. Flow chart of the control algorithm.

V. CURRENT RIPPLE ANALYSIS

To maintain ZCS operation, energy injection needs to be in half period. Due to the discrete nature, the energy injected in the resonant tank may be higher or lower than the actual load consumption, and as such, the primary current will exhibit some ripple during operation. For analysis and design purposes, it is important to quantify the magnitude of the current ripple. Because the extent of the current ripple is load dependent, and it varies with energy injection instants, it is very difficult to conduct accurate ripple analysis under all the operating conditions of the inverter. However, a worst-case analysis approach is possible to find the maximum and minimum currents, which quantifies the worst ripple the inverter can have.

The maximum peak current i_{L_max} occurs under the condition when there is no load, and the current peak in the previous half cycle is slightly smaller than or just equal to the reference value $-I_{ref}$, so that energy is injected into the resonant network in the next half cycle. The current waveform under such a worst case condition is shown in Fig. 6.The maximum current i_{L_max} appears in the following half cycle

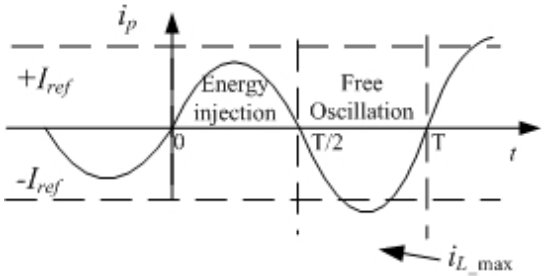

Fig. 6. Maximum track current under worst case condition.

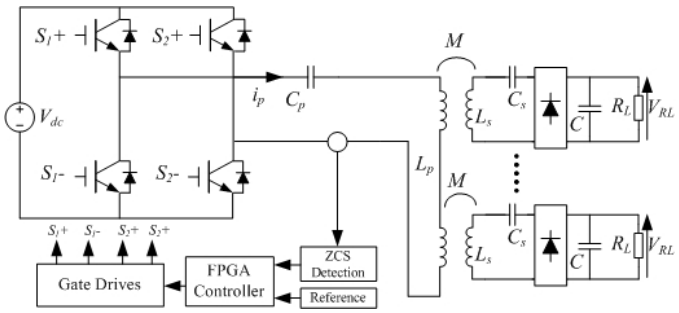

Fig. 7. System configuration for experiment.

after the energy injection.

Because there is no load, the capacitor voltage is zero when the track current is at its peak. The total energy stored in the resonant circuit before the energy injection can be expressed as:

$$E_{store} = \frac{1}{2} L \hat{I}_{ref}^{\ 2}. \tag{11}$$

After energy injection over half a period, the total energy storage in the circuit becomes:

$$\frac{1}{2} L \hat{i}_{L\_\max}^{\ 2} = \frac{1}{2} L \hat{I}_{ref}^{\ 2} + E_{in}. \tag{12}$$

The amount of injected energy is determined by the magnitude of the input dc voltage and the track current governed by (8), where (assuming ZCS operation is required) the period of the energy injection is half of the period of the resonant track current. According to (7), the maximum current during energy injection can be expressed as:

$$\hat{i}_L = \frac{V_d - V_c(0)}{\omega L} e^{\frac{-T}{4\tau}}. \tag{13}$$

Here $V_c(0)$ is the initial value of the capacitor voltage at $t = 0$, which can be determined by:

$$V_c(0) == \sqrt{\frac{L}{C}} I_{ref}. \tag{14}$$

From (13) and (14), the injected energy in half period can be expressed as:

$$E_{in} = V_d \int_0^{\frac{T}{2}} i_L(t) dt = \frac{T V_d (V_d + \sqrt{\frac{L}{C}} I_{ref})}{Z\pi}. \tag{15}$$

Substituting (15) into (12), the maximum current can be expressed as:

$$\hat{i}_{L\_\max} = \sqrt{I_{ref}^2 + \frac{2TV_d}{\pi} + \sqrt{\frac{C}{L}} \frac{2TV_d^2}{\pi I_{ref}}}. \tag{16}$$

(16) shows that the worst case track current overshoot above its reference value is determined by the input voltage, the track current oscillation frequency, and the circuit parameters.

The minimum current i_{L_min} is caused by circuit damping. The worst case scenario arises when the load is at its maximum and the peak current is slightly larger than the reference value, consequently there is no injection in the next half cycle the current magnitude would decay continuously. Starting from $i(0) = -I_{ref}$ and $v_c(0) = 0$, equation (4) can be further expressed as:

$$i_L(t) = -I_{ref} \frac{\omega_0}{\omega} e^{-\frac{t}{\tau}} \cos(\omega t + \theta). \tag{17}$$

Note that strictly speaking when the current is at its peak, the capacitor voltage is not exactly zero due to the existence of the load. However, for inductive power transfer applications, the primary circuit Q is usually high so the error caused by this assumption is naturally very small.

For a full bridge topology, the current reaches its minimum value after half a period from the previous peak value, so i_{L_min} can be expressed as:

$$\hat{i}_{L\_\min} = I_{ref} \frac{\omega_0}{\omega} e^{-\frac{RT}{4L}}. \tag{18}$$

From (18), it can be seen that the worst case minimum is determined by the load, the track current oscillation frequency, and the circuit parameters.

VI. Experimental Results

In order to evaluate the performance of the proposed controller at a system level, a number of series tuned power pickups, which are coupled with the primacy circuit, are considered. In practical applications many different types of power pickups can be used, for simplicity only series tuned pickups are considered. Fig. 7 shows the circuit diagram of the system being studied. To realize the proposed control strategy with fast sampling and minimal delay, a FPGA controller is designed and implemented to achieve ZCS operation. The detailed circuit parameter of the system is listed in Table II.

Fig. 8 shows the start-up transient response operation of the proposed inverter. It can be seen that at the beginning S_1+ is kept "on" for a short period (S_2- is also "on" but not shown). Once the voltage of the capacitor C_p equals to the input voltage, S_1+ and S_2+ both turned off (S_2- and S_1- are turned "on"), and an oscillation path is formed so that the current oscillates freely in the track. After the initial forced energy injection and first half cycle oscillation, S_1+ (trace4) turns "on" in each positive half cycle and S_2+ (trace3) turns "on" in each negative half cycle to ensure the maximum energy injection to boost the current to the reference ±15A as fast as possible. Once the peak track current reaches a predefined reference, the switching frequency decreases to reduce the energy injection and maintain the track current relatively constant. The duration of the start-up transient to steady-state takes only a few cycles from the experiment, which here has a single pickup coupled at the start-up with nominal load. A higher source voltage and/or a lighter load will make the start-up process faster, but the overshoot and fluctuations of the track current at steady-state will become slightly higher due to the ZCS operation.

TABLE II
CIRCUIT PARAMETERS

Notes	Symbol	Value
Input dc voltage	V_{dc}	24V
Primary track/coil inductance	L	67.81 μH
Secondary coil inductance	L_s	45.16 μH
Primary tuning capacitance	C	0.88 μF
Secondary tuning capacitance	C_s	1.36 μF
Coupling coefficient	k	0.138
Nominal load resistance of one pickup	R_L	2 Ω
Nominal system frequency	f	20 kHz
Reference peak current	I_{ref}	15 A

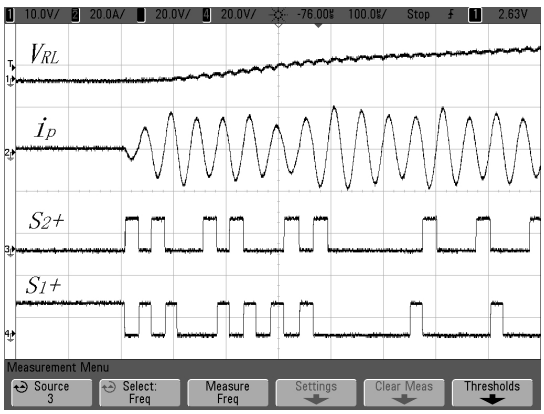

Fig. 8. The transient response of the proposed inverter on start-up.

Fig. 8 shows the start-up transient response operation of the proposed inverter. It can be seen that at the beginning S_1+ is kept "on" for a short period (S_2- is also "on" but not shown). Once the voltage of the capacitor C_p equals to the input voltage, S_1+ and S_2+ both turned off (S_2- and S_1- are turned "on"), and an oscillation path is formed so that the current oscillates freely in the track. After the initial forced energy injection and first half cycle oscillation, S_1+ (trace4) turns "on" in each positive half cycle and S_2+ (trace3) turns "on" in each negative half cycle to ensure the maximum energy injection to boost the current to the reference $\pm$15A as fast as possible. Once the peak track current reaches a predefined reference, the switching frequency decreases to reduce the energy injection and maintain the track current relatively constant. The duration of the start-up transient to steady-state takes only a few cycles from the experiment, which here has a single pickup coupled at the start-up with nominal load. A higher source voltage and/or a lighter load will make the start-up process faster, but the overshoot and fluctuations of the track current at steady-state will become slightly higher due to the ZCS operation.

The steady-states operation is shown in the later part of Fig. 9. Here the track current frequency is close to the nominal resonant frequency that all pickup are tuned to operate at. Under the control strategy the inverter has a good dynamic response. The high frequency track current is generated, and its magnitude is maintained around the reference level despite the low switching operation. It can be seen from Fig. 9 that small fluctuations in current arise because of the fast energy consumption of the load during the free oscillation period, and a slight over energy injection during the half period of energy injection, which is limited by the half period energy injection if the ZCS condition is maintained. Fig. 9 shows that the practical experimental value of the maximum current

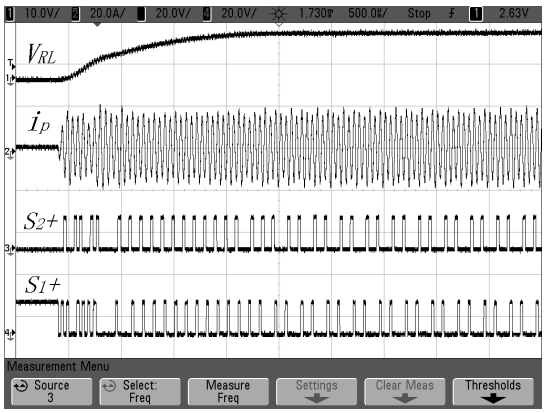

Fig. 9. The response from start-up to steady state.

is about 19A, which is smaller than the theoretical worst case value of 20.47A calculated from (16). The practical minimal current obtained is about 14A, which is also within theoretical limit of 13.74A calculated from (18). It can also be seen from Fig. 9 that practically these track current fluctuations have very minimal effect on the output voltage, because nearly all contactless power transfer applications have some form of capacitor filtering or bulk storage at the output (as in Fig. 1) which contains sufficient energy to supply the load over many resonant cycles. In addition, if necessary, the fluctuations can be minimized or eliminated by controlling the energy injection using a hard switching strategy, or a combined hard/soft switching approach, but in either case full ZCS will be compromised, which is not desired here.

In order to investigate the proposed control method for the applications with multiple pickups, an experiment is undertaken with same specification in Table II but with two identical pickups. Fig. 10 shows the experimental results. From top to the bottom, the waveforms are V_{RL1} of one of the identical pickup, S_1+, S_2+ and the primary current. In the beginning both pickups are fully loaded and the system operates at steady state. After 5ms in Fig. 10, both pickups are decoupled from the track (indicating no energy is desired) in order to evaluate the response of the inverter. At this point the voltage over the load V_{RL1} on one of the pickups is shown to drop to zero Fig. 10 (trace1). The inverter now only operates to overcome the track losses and maintain the current on the primary resonant circuit. As a result, all switches operate at low switching frequencies and the switch pattern is different. In Fig. 10, only S_1+ is operating, S_2+ is standing by under this "no load" condition. In practice, the switching pattern is related to the reference value of the track current and the loading condition, which is difficult to predict.

In order to investigate the proposed control method for the applications with multiple pickups, an experiment is undertaken with same specification in Table II but with two identical pickups. Fig. 10 shows the experimental results. From top to the bottom, the waveforms are V_{RL1} of one of the identical pickup, S_1+, S_2+ and the primary current. In the beginning both pickups are fully loaded and the system operates at steady state. After 5ms in Fig. 10, both pickups are decoupled from the track (indicating no energy is desired) in order to evaluate the response of the inverter. At this point the voltage over the

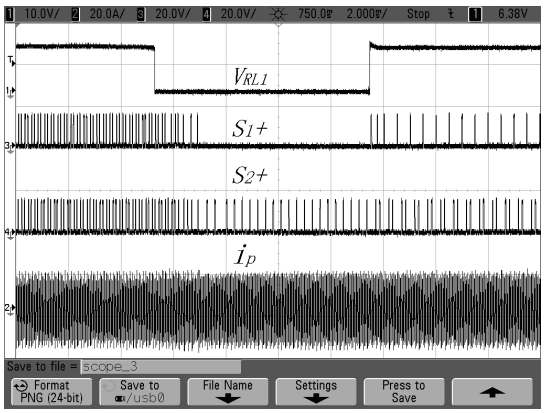

Fig. 10. Load variations from two pickups to no pickup and one pickup.

load V_{RL1} on one of the pickups is shown to drop to zero Fig. 10 (trace1). The inverter now only operates to overcome the track losses and maintain the current on the primary resonant circuit. As a result, all switches operate at low switching frequencies and the switch pattern is different. In Fig. 10, only S_1+ is operating, S_2+ is standing by under this "no load" condition. In practice, the switching pattern is related to the reference value of the track current and the loading condition, which is difficult to predict.

At around 13ms in Fig. 10, one of the pickups is re-coupled to the track demanding full power while the other remains decoupled. It can be seen that V_{RL1} on the resistor increases very fast compared to the cold start-up transient as shown in Fig. 8. This is because the dc capacitor at the output of the rectifier is charged and enables immediate power transfer. The stored energy on dc capacitor helps to boost the voltage when load presents. It can be seen that the switches operate in a different pattern again, when only one fully loaded pickup is presented. The switching frequencies of both S_1+ and S_2+ increase compared to the no load condition. However, the magnitude of the primary current is still maintained near the preset reference value under all operation conditions. Furthermore, the transient overshoots of the primary current which exist as a result of the energy injection are naturally limited, which can be well predicted as discussed in the ripple analysis.

The track current waveforms obtained are sufficiently good for contactless power transfer applications. The primary current is fully controllable and can be maintained around the preset reference value under light load or even no-load conditions. However, as such contactless power transfer systems may present a lower efficiency under lightly loaded conditions, most of the injected energy is required to compensate for the standing power losses rather than to transfer power to secondary sides. The power efficiency of the measured system is shown in Fig. 11 over the entire load range.

It can be seen that it is only about 30% efficiency when the load resistance is 12.35Ω at 11W. It is about 70% power efficiency at nominal single pickup load condition at 60W in Table II. A higher power efficiency is achieved in a multiple pickups system. The measured power efficiency is about 82% for a two pickups system in which each pickup has a nominal load (120W in total) at the 0.138 coupling coefficient, as the

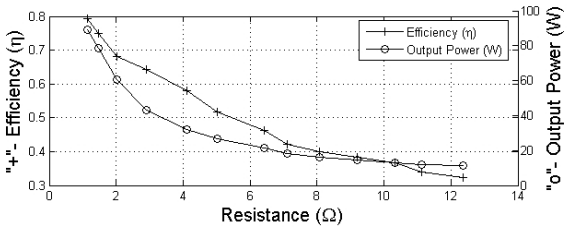

Fig. 11. Power efficiency and output power over the load rang of a single pickups system.

standing power losses take less portion of total power. In fact, for a multiple pickups system, usually there are more than one pickup coupled to the primary, therefore the average efficiency of multiple pickups system is normally higher than a signal pickup at same coupling condition. Consequently, the total power efficiency of the proposed inverter can still be very high for such multiple pickups applications. In addition, the standing losses of the system can be reduced by a proper circuit design [22], by an accurate control timing of switches, or choosing better components, such as Litz wire coils, etc.

VII. Conclusions

In this paper, a high frequency current generation and control method is proposed for contactless power transfer applications based on free oscillation and energy injection control principles. Theoretical modelling and analysis are conducted to understand the operation of the proposed method. A ZCS strategy has been proposed to control the full bridge inverter, which has been verified by simulation and experimental studies. A FPGA based controller is developed as the core control unit to implement the control strategy so as to achieve fast and accurate ZCS operation. Experimental results have demonstrated that the proposed inversion method is able to generate a high frequency output current at a low switching frequency. The inverter operates at full ZCS and has very good start-up and steady-state properties. Furthermore, the primary current ripples that arise during operation have been analysed, and it has been found that the actual magnitude of the current ripple is very small, and has little impact on the secondary power pickup output.

References

[1] M. Budhia, V. Vyatkin, and G. A. Covic, "Powering flexible manufacturing systems with intelligent contact-less power transfer," in 6th IEEE International Conference on Industrial Informatics, pp. 1160-1165, 2008.

[2] S. Y. R. Hui and W. W. C. Ho, "A new generation of universal contactless Battery Charging platform for portable Consumer Electronic equipment," IEEE Trans. on Power Electron., Vol. 20, pp. 620-627, 2005.

[3] J. A. A. Qahouq, O. Abdel-Rahman, L. Huang, and I. Batarseh, "On load adaptive control of voltage regulators for power managed loads: Control schemes to improve converter efficiency and performance," IEEE Trans. on Power Electron., Vol. 22, No. 5, pp. 1806-1819, Sep. 2007.

[4] Y. Wu, L. Yan, and S. Xu, "A new contactless power delivery system," in 6th International Conference on Electrical Machines and Systems, pp. 253-256, 2003.

[5] L. Zhao, C. F. Foo, K. J. Tseng, and W. K. Chan, "Transcutaneous transformers in power supply system for an artificial heart," in International Conference on Power Electronic Drives and Energy Systems for Industrial Growth, pp. 348-352,1998.

[6] R. Mecke and C. Rathge, "High frequency resonant inverter for contactless energy transmission over large air gap," in IEEE 35th Annual Power Electronics Specialists Conference, pp. 1737-1743, 2004.

[7] Y. Su, C. Tang, S. Wu, and Y. Sun, "Research of LCL resonant inverter in wireless power transfer system," in International Conference on Power System Technology, pp. 1-6, 2006.

[8] J. J. Casanova, L. Zhen Ning, and L. Jenshan, "Design and optimization of a class-e amplifier for a loosely coupled planar wireless power system," IEEE Trans. Circuits Syst. II, Exp. Briefs, Vol. 56, No. 11, pp. 830-834, Nov. 2009.

[9] Y. Su, C. Tang, S. Wu, and Y. Sun, "Research of lcl resonant inverter in wireless power transfer system," in International Conference on Power System Technology (PowerCon 2006), pp. 1-6, 2006.

[10] L. QingFeng, W. HuaMin, and L. ZhaoXia, "Discuss on the application of multilevel inverter in high frequency induction heating power supply," in IEEE Region 10 Conference, pp. 1-4, 2006.

[11] Z. Wenqi and M. Hao, "Dynamic analysis of a current source inductively coupled power transfer system," in CES/IEEE 5th International Power Electronics and Motion Control Conference, pp. 1-5, 2006.

[12] Q. Chen, S. C. Wong, C. K. Tse, and X. Ruan, "Analysis, design and control of a transcutaneous power regulator for artificial heart," in IEEE Power Electronics Specialists Conference, pp. 1833-1838, 2008.

[13] A. P. Hu, G. A. Covic, and J. T. Boys, "Direct ZVS start-up of a current-fed resonant inverter," IEEE Trans. on Power Electron., Vol. 21, No. 3, pp. 809-812, May 2006.

[14] S. V. Mollov, M. Theodoridis, and A. J. Forsyth, "High frequency voltage-fed inverter with phase-shift control for induction heating," IEE Proceedings on Electric Power Applications, Vol. 151, No. 1, pp. 12-18, Jan. 2004.

[15] H. L. Li, A. P. Hu, and G. A. Covic, "FPGA controlled high frequency resonant converter for contactless power transfer," in Power Electronics Specialists Conference, Rhodes, pp. 3642-3647, 2008.

[16] A. P. Hu and L. Hao Leo, "A new high frequency current generation method for inductive power transfer applications," in Power Electronics Specialists Conference, pp. 1-6, 2006.

[17] G. B. Joung, J. G. Cho, and G. H. Cho, "A generalized quantum resonant converter using a new quantum resonant module," IEEE Trans. on Power Electron., Vol. 7, No. 4, pp. 666-672, Oct. 1992.

[18] W. H. Kwon and G. H. Cho, "Optimum quantum sequence control of quantum series resonant converter for minimum output voltage ripple," IEEE Trans. on Power Electron., Vol. 9, No. 1, pp. 74-84, Jan. 1994.

[19] C.-S. Wang, O. H. Stielau, and G. A. Covic, "Load models and their application in the design of loosely coupled inductive power transfer systems," in Proceedings International Conference on Power System Technology, pp. 1053-1058, 2000.

[20] D. B. Geselowtiz, Q. T. N. Hoang, and R. P. Gaumond, "The effects of metals on a transcutaneous energy transmission system," IEEE Trans. Biomed. Eng., Vol. 39, No. 9, pp. 928-934, sep. 1992.

[21] C.-S. Wang, G. A. Covic, and O. H. Stielau, "Power transfer capability and bifurcation phenomena of loosely coupled inductive power transfer systems," IEEE Trans. on Ind. Electron., Vol. 51, No. 1, pp. 148-157, Feb. 2004.

[22] S. Valtchev, B. V. Borges, and J. B. Klaassens, "Contactless energy transmission with optimal efficiency," in IECON 02, pp. 1330-1335, Vol. 2, 2002.

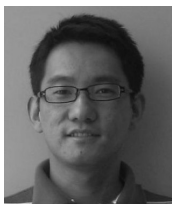

Hao Leo Li was born in GuiZhou, China. He received the B.E. degree in electrical engineering from the GuiZhou University in 2002. He received his M.E. and is currently pursuing a PhD in the Department of Electrical and Computer Engineering, the University of Auckland. He is engaged in research on power electronics, contactless power transfer, and resonant power converters.

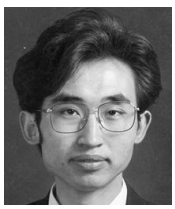

Aiguo Patrick Hu (M'1998, SM'2007) graduated from Xian JiaoTong University, China, with BE and ME degrees in 1985 and 1988 respectively. After migrating to New Zealand in 1996 he received his Ph.D from the University of Auckland in 2001. Before that he worked as a lecturer, director of China Italy Cooperative Technical Training center in Xian, and later the general manager of a technical development company. He holds 5 patents in inductive power transfer and microcomputer control technologies, published more than 70 referred journal and conference papers, authored a monograph on wireless/contactless power transfer, and contributed book chapters on electrical machines and inductive power transfer control. He is currently with the Department of Electrical and Electronic Engineering, the University of Auckland. His research interests include contactless/wireless power transfer, power converters, and application of power electronics in renewable power systems.

Grant Anthony Covic (S'88–M'89–SM'04) received the B.E. (Hons.) and the Ph.D. degrees from The University of Auckland, Auckland, New Zealand, in 1986 and 1993 respectively. He was a Full-time Lecturer in 1992, a Senior Lecturer in 2000, and an Associate Professor in 2007 with the Department of Electrical and Computer Engineering, The University of Auckland, where he is currently the Head of the power research cluster in the Faculty of Engineering. He has authored or coauthored more than 80 papers in international journals and conferences and holds a number of patents in the field of inductive (contactless) power transfer (IPT). His research interests include power electronics and IPT.